

Effect of heat treatment on bioactivity and mechanical properties of PDMS-modified CaO-SiO₂-TiO₂ hybrids via sol-gel process

Q. CHEN¹, N. MIYATA¹, T. KOKUBO^{1*}, T. NAKAMURA²

¹Department of Material Chemistry, Faculty of Engineering, Kyoto University, Yoshida-Honmachi, Sakyo-ku, Kyoto 606–8501, Japan

²Department of Orthopaedic Surgery, Faculty of Medicine, Kyoto University, Shogoin-Kawaharacho, Sakyo-ku, Kyoto 606–8507, Japan

E-mail: Kokubo@sung7.kuic.kyoto-u.ac.jp

Crack- and pore-free transparent monolithic disks of polydimethylsiloxane (PDMS)- modified CaO-SiO₂-TiO₂ hybrids were obtained by hydrolysis and polycondensation of PDMS, tetraethoxysilane, tetraisopropyltitanate and calcium nitrate. The product as-dried at 60 °C formed an apatite on its surface in a simulated body fluid (SBF) within only one day, indicating its high bioactivity. The apatite-forming ability decreased slightly by a heat treatment below 250 °C. The bending strength of the product was about 11 MPa, independent of the heat treatment. This average strength value is comparable to that of the human cancellous bone. Young's modulus of the products increased from 100 to 500 MPa with increasing heat treatment temperature from 60 to 250 °C, but its values were within the range of those of the human cancellous bone. The strain at failure of the products decreased with increasing heat treatment temperature. Failure strains went down to the magnitudes exhibited by the human cancellous bone, when the products were heat treated in the temperature range from 150 to 250 °C. Thus, highly bioactive hybrids with mechanical properties analogous to those of the human cancellous bone were obtained. This new kind of bioactive hybrid may be useful as a bone-repairing material.

© 2001 Kluwer Academic Publishers

1. Introduction

Researchers in the past three decades have shown that some ceramics, such as Na₂O-CaO-SiO₂-P₂O₅ glasses [1], sintered hydroxyapatite [2] and glass-ceramics containing crystalline apatite and wollastonite [3], can bond to living bone. They are already clinically used as important bone-repairing materials. Recently, it was also revealed that even metals, such as titanium and its alloys can bond to living bone, if they were previously subjected to alkali and heat treatments [4]. They have, however, higher elastic moduli than those of the natural bone. On the other hand, polymeric materials generally have low elastic moduli, but they are not bioactive, except for Polyactive[®] which is biodegradable [5]. The development of new types of materials having not only high bioactivity but also mechanical properties analogous to those of the natural bone is very important.

Organically modified sol-gel derived ceramics are currently attracting much attention because of their unique properties, such as high extensibilities and low elastic moduli combined with high mechanical strengths. In these hybrid materials, organic component is chemically incorporated into inorganic network at

molecular level [6–13]. They are called “ormosil” or “ceramer” and can be candidates as a new kind of bioactive bone-repairing material. However, few works have been published on the bioactivity of the hybrids. Tsuru *et al.* [14] reported recently that a kind of organically modified silica heated at 60 °C forms an apatite on its surface in a simulated body fluid (SBF) with ion concentrations nearly equal to those of the human blood plasma, when it contains a certain amount of calcium ion. This indicates that the ormosil can be bioactive. It was revealed by the present authors [15] that incorporation of titanium oxide into the polydimethylsiloxane (PDMS)-modified silica network gives wide variation in the mechanical properties of the hybrids and excellent bioactivity. PDMS itself is known to be stable up to 150 °C [16]. However, effects of heat treatment on the properties of PDMS-modified CaO-SiO₂-TiO₂ hybrids are not yet revealed.

In the present work, the polydimethylsiloxane-modified CaO-SiO₂-TiO₂ hybrids prepared by sol-gel method were subjected to various heat treatments. Effects of the heat treatments on the bioactivity and mechanical properties of the products were investigated.

*Author to whom all correspondence should be addressed.

2. Materials and methods

2.1. Material and preparation

Tetraethoxysilane (TEOS, $\text{Si}(\text{OC}_2\text{H}_5)_4$), tetrakispropyltitanate (TiPT, $\text{Ti}(\text{OCH}(\text{CH}_3)_2)_4$), calcium nitrate ($\text{Ca}(\text{NO}_3)_2 \cdot 4\text{H}_2\text{O}$) and hydrochloric acid (HCl 35%) (Nacalai tesque Inc., Kyoto, Japan) were used as starting inorganic constituents. Polydimethylsiloxane (PDMS, $\text{HO}[\text{Si}(\text{CH}_3)_2\text{O}]_n\text{H}$, Aldrich Chemical Co., Milwaukee, USA) with average molecular weight of 1100 was used as the organic component. Molar ratio of TEOS and TiPT was kept constant at 9:1. The molar ratios of the water, PDMS and calcium nitrate to the metal alkoxides were kept at 2.0, 0.11 and 0.15, respectively. TEOS was first pre-hydrolyzed in aqueous solution containing iso-propyl-alcohol (IPA) and tetrahydrofuran (THF), and the catalyst 35% HCl. After reacting for two hours, a given amount of PDMS was added to the solution. Fifteen hours later, TiPT and a mixture of $\text{Ca}(\text{NO}_3)_2 \cdot 4\text{H}_2\text{O}$, H_2O and IPA were mixed with the former solution. The aging of the solutions was performed in a covered plastic container at ambient condition for one day. After partial evaporation of the solvents, they were kept at 40 °C for gelation for seven days. Monolithic disks of approximately 70 mm diameter and 6 mm thickness were obtained. The obtained products were heated up to 60 °C at a rate of 1 °C /min, and held at 60 °C for three days or heated up to various temperatures below 300 °C at a rate of 1 °C /min, and held at the respective temperature for 24 h, and allowed to be cooled in the furnace.

2.2. Characterization

Thermal stability of the product as-dried at 60 °C for three days was measured by differential thermal analysis (DTA) and thermo-gravimetric analysis (TGA) in air at a heating rate of 5 °C /min (Model 8112BH, Rigaku Co., Tokyo, Japan). The pore size distributions of the products were measured by the mercury intrusion method (PORESIZER 9320, Micromeritics, Norcross, USA). The structural groups in the products were analyzed by Fourier transform infra-red (FTIR) absorption spectroscopy (FTIR 5M, JASCO, Tokyo, Japan) using KBr tablets.

2.3. Soaking in simulated body fluid (SBF)

Bioactivities of the products were evaluated by examining apatite formation on their surfaces in SBF [17]. The specimens of $10 \times 10 \times 2 \text{ mm}^3$ in size were cut and polished with a #400 abrasive disk, washed with distilled water and dried at 40 °C. SBF with inorganic ion concentrations (in mM: Na^+ 142, K^+ 5.0, Mg^{2+} 1.5, Ca^{2+} 2.5, Cl^- 147.8, HCO_3^- 4.2, HPO_4^{2-} 1.0, SO_4^{2-} 0.5) nearly equal to those of human blood plasma was prepared by dissolving reagents NaCl, NaHCO_3 , KCl, $\text{K}_2\text{HPO}_3 \cdot 3\text{H}_2\text{O}$, $\text{MgCl}_2 \cdot 6\text{H}_2\text{O}$, CaCl_2 , and Na_2SO_4 (Nacalai tesque Inc., Kyoto, Japan) in distilled water and buffered to pH 7.4 at 36.5 °C with $(\text{CH}_2\text{OH})_3\text{CNH}_2$ and 1 M HCl (Nacalai tesque Inc., Kyoto, Japan). It is confirmed for various materials that materials which form an apatite on their surfaces in this SBF also form the apatite in the living body and bond to living bone

[18, 19]. The specimens were soaked in 30 ml of SBF at 36.5 °C. After soaking in SBF for various periods, the specimens were removed from the fluids, washed moderately with ion-exchanged distilled water, and dried at 40 °C for one day.

2.4. Analysis of the specimen surface and element concentrations of SBF

The surfaces of the specimens were analyzed by thin-film X-ray diffraction (TF-XRD: Model 2651A, Rigaku Co., Tokyo, Japan) and Fourier transform infra-red reflection spectroscopy (FTIRRS: Model System 2000, Perkin-Elmer, Beaconsfield Bucks, UK). In the TF-XRD, the surface of the samples was fixed at an angle of 1 °C against the direction of the incident beam. This technique enables the detection of a surface layer about 1 μm thick. The surfaces of the specimens were examined using a scanning electron microscope (SEM: Model S2500CX, Hitachi Ltd, Tokyo, Japan) after coating a thin Au-Pd film.

Changes in element concentrations of SBF due to the soaking of the specimens were measured with inductively coupled plasma (ICP) atomic emission spectroscopy (Model SPS1500, Seiko Inst., Japan).

2.5. Measurement of mechanical property

Rectangular bar specimens of $3 \times 4 \times 30 \text{ mm}^3$ in size were cut from the disks and polished with #2000 diamond paste. Bending test of the specimens was carried out with an Instron-type testing machine (Model AGS-10kNG, Shimadzu Co. Ltd, Kyoto, Japan) using a three-point loading over a 20 mm span at a crosshead speed of $0.5 \text{ mm} \cdot \text{min}^{-1}$. All measurements were made in air at room temperature. Eight specimens were tested for each composition. The Young's modulus was determined from the slope of the initial linear elastic portion of the load-deflection curve, loading geometry and specimen dimensions on the basis of the simple linear elastic beam analysis. For materials having linear or approximately linear behavior up to the point of fracture, the maximum tensile edge stress and strain were calculated from the load and deflection data using simple elastic beam theory. For materials which exhibit the large non-linear portion in the load-deflection curve, corrections were made based on the assumption that, beyond the initial linear portion, stress is approximately proportional to strain raised to a power. The exponent was estimated from a logarithmic plot of the experimental load-deflection data. The failure strain and ultimate strength of the specimens were thus evaluated. It is possible that the neutral axis may shift somewhat from the centroid of the cross-sectional area of the beam as deformation largely progresses, but this was not taken into account in the present calculations.

3. Results

3.1. Structure of the products

The product heat treated at 60 °C was homogeneous and transparent, without causing a cracking problem, which is often observed in oxide ceramics. The color of the

TABLE I Properties of the hybrids heat treated at various temperatures

| Heat treatment temperature (°C) | Appearance | Apatite formation in SBF | | | | | |
|---------------------------------|--------------------------|--------------------------|-----|-----|-----|------|------|
| | | 0.5 d | 1 d | 3 d | 7 d | 14 d | 28 d |
| 60 | Pale yellow, transparent | — | ○ | ○ | ○ | ○ | ○ |
| 100 | Pale yellow, transparent | — | — | ○ | ○ | ○ | ○ |
| 150 | Yellow, transparent | — | — | ○ | ○ | ○ | ○ |
| 200 | Light brown, transparent | — | — | ○ | ○ | ○ | ○ |
| 250 | Brown, transparent | — | — | ○ | ○ | ○ | ○ |
| 300 | Brown, opaque, cracked | — | — | ○ | ○ | ○ | ○ |

products changed from pale yellow to brown, as the heat treatment temperature increased from 60 to 300 °C, as shown in Table I. The products heat treated below 250 °C were transparent and crack free, whereas those heat treated at 300 °C were opaque and cracked. Fig. 1 shows the cumulative pore volume and pore size distribution curves of the products heat treated at 60 and 150 °C, respectively. The pore volume and the average diameter of pores were very small for both products. The pore volume of the products heat treated at 200 and 250 °C was too small to be detected by the present method.

Fig. 2 shows the DTA-TGA curve of the as-dried product. Gradually increasing exothermic weight loss behavior was observed from the starting temperature of DTA-TGA analyses, giving a sharp exothermic peak and large weight loss at 500 °C. These changes might be due to release of PDMS.

Fig. 3 shows the IR absorption spectra of the products heat treated at various temperatures. The absorption peak at 805 cm⁻¹ was assigned to Si-C bonds, peaks at 850 cm⁻¹ and 950 cm⁻¹ to Si-OH bonds, peak at 930 cm⁻¹ to Si-O-Ti bonds, peak at 1080 cm⁻¹ to Si-O-Si bonds, peak at 1260 cm⁻¹ to C-H vibrations of Si-CH₃ bonds, peak at 1390 cm⁻¹ to C-H stretching vibrations, and peak at 1640 cm⁻¹ to H-OH bonds [19–25]. The IR absorption spectra of the products changed slightly with the heat treatment temperature, except for the peak at 1390 cm⁻¹ being ascribed to C-H stretching vibrations, the intensity of which decreased with increasing heat treatment temperature. These indicate that the products are essentially composed of a Si-O-Ti network modified

with methyl groups, irrespective of the heat treatment temperature. Only the content of PDMS decreases with increasing heat treatment temperature.

3.2. Bioactivity of the products

Figs 4 and 5 show TF-XRD patterns and FTIR reflection spectra of the surfaces of the products heat treated at various temperatures, before and after soaking in SBF for up to 28 days. The 1260 and 805 cm⁻¹ peaks in the FTIR reflection spectra are ascribed to CH₃ and Si-C vibrations, respectively [23, 24]. Si-O stretching vibration was observed at 1110 cm⁻¹. The peak at 470 cm⁻¹ was assigned to the O-Si-O bending vibration. Peaks at 1060 and 1130 cm⁻¹ were assigned to P-O stretching vibration; 560 and 610 cm⁻¹ peaks to P-O bending mode [19, 26]. Figs 6 and 7 show SEM photographs of the surfaces of the products heat treated at various temperatures, before and after soaking in SBF for seven days. The apatite formation on their surfaces in SBF, which was determined by TF-XRD for each sample, is shown in Table I. It can be seen from Figs 4 through 7 and Table I that the product heat treated at 60 °C forms the apatite within one day and the products heat treated at 100 to 250 °C form the apatite within three days.

Fig. 8 shows changes in element concentrations of SBF with soaking of the products heat treated at 60, 150 and 250 °C. Titanium was not detected in SBF up to 28 days. All the products showed increases in the calcium and silicon concentrations and a decrease in the phosphorus concentration. The magnitudes of the

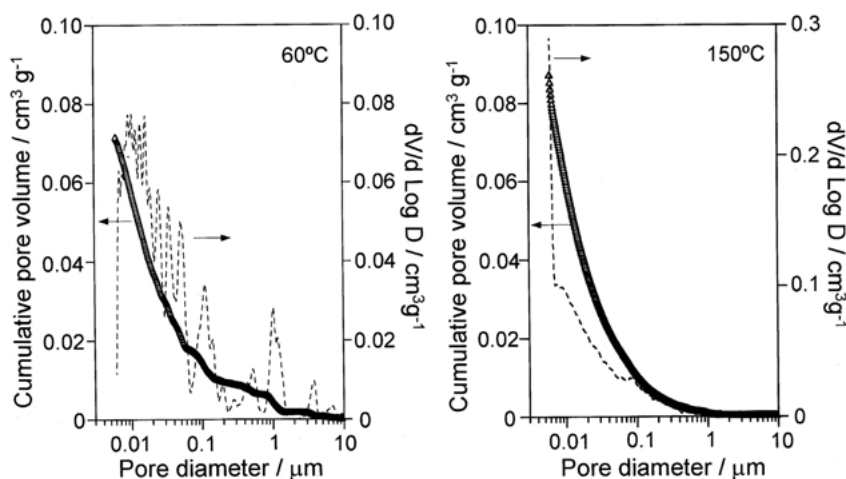


Figure 1 Cumulative pore volume and pore size distribution of the products heat treated at 60 and 150 °C.

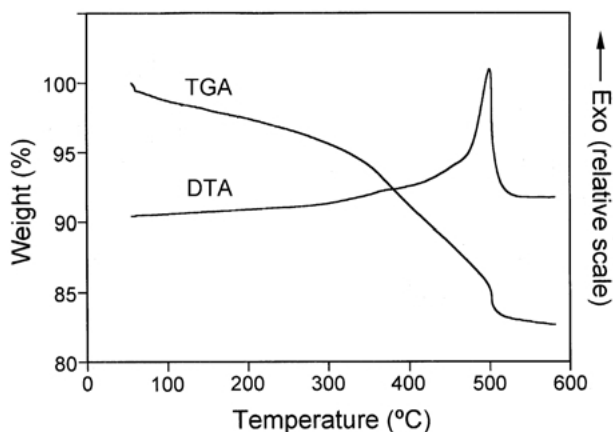


Figure 2 DTA and TGA curves of the as-dried product.

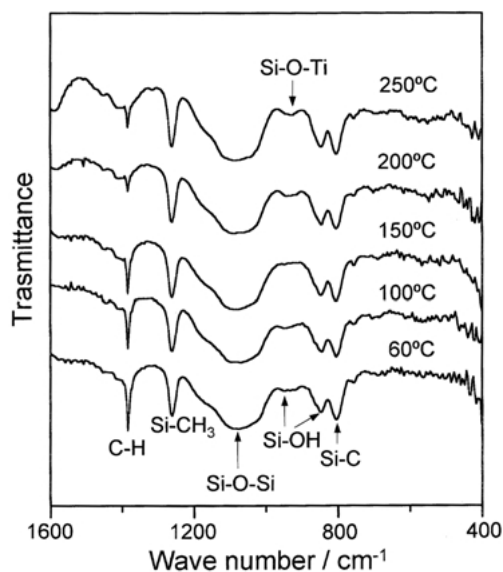


Figure 3 FTIR absorption spectra of the products heat treated at various temperatures.

increases in the calcium and silicon concentrations decreased with increasing heat treatment temperature.

3.3. Mechanical properties of the products

In Fig. 9, representative stress versus strain curve from three-point bending test is shown for each of the products heat treated at 60, 150 and 250 °C. The bending strengths

were around 11 MPa, independent of the heat treatment temperature. It can be seen from Fig. 9, that unlike usual brittle ceramics, a large extension occurs in all the samples although its degree varies with the samples. The strain at failure which is a measure of capability for deformation, decreased with increasing heat treatment temperature, i.e. 32, 14 and 2.2% for the products heat treated at 60, 150 and 250 °C, respectively. The Young's modulus evaluated from the slope of the initial linear elastic portion of the load-deflection curve are shown in Fig. 10 as a function of heat treatment temperature. The range of Young's moduli of human cancellous bone [27] is also drawn in Fig. 10 for comparison. The Young's modulus is found to increase with increasing heat treatment temperature.

4. Discussion

The results described above showed that the crack free and essentially pore free transparent monolithic products are successfully obtained by the sol-gel process. These products were stable up to 250 °C, although their color slightly changed from pale yellow to brown with increasing heat treatment temperature. This color change might be attributed to a partial reduction of the titanium ion involved.

It has been shown that polycondensation of hydrolyzed TEOS and PDMS with the terminal Si-OH groups results in an interconnected network in which condensed silicate islands (from TEOS), surrounded and chemically bonded by flexible organic $[-Si(CH_3)_2O-]$ chains at molecular levels [28–30]. It is speculated that TiO_4 groups could be incorporated into the SiO_4 groups, when TiPT is added to this system. When the calcium ion is added to this system, it is assumed that the Ca^{2+} ion is ionically bonded with the O^- ion of the SiO_4 and TiO_4 groups. It is confirmed from Fig. 3 that such structural groups as Si-CH₃, Si-O-Si, Si-O-Ti are present in the present products. According to Fig. 3, Si-OH groups are also present in the products. It should be noted that such structure of PDMS-modified CaO-SiO₂-TiO₂ hybrids is already formed at 60 °C, and essentially does not change with heat treatment at higher temperatures below 250 °C. Only a small amount of PDMS decreases with increasing heat treatment temperature, as shown in Figs 2 and 3.

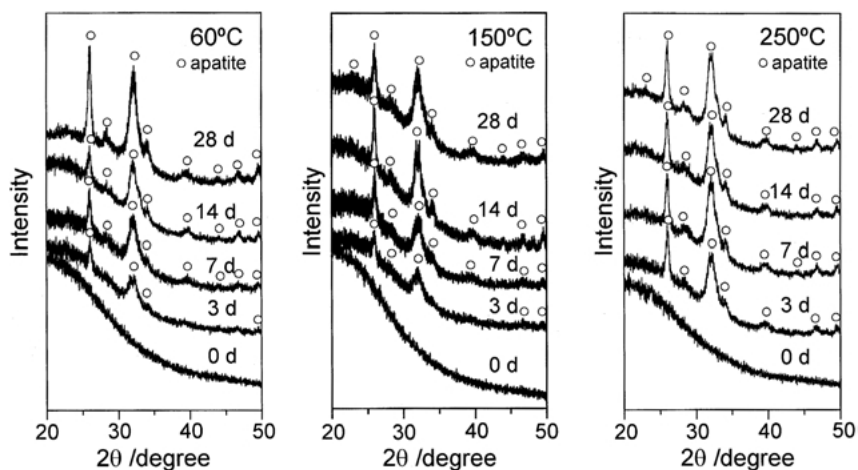


Figure 4 TF-XRD patterns from the surfaces of the products heat treated at 60, 150 and 250 °C and soaked in SBF for various periods.

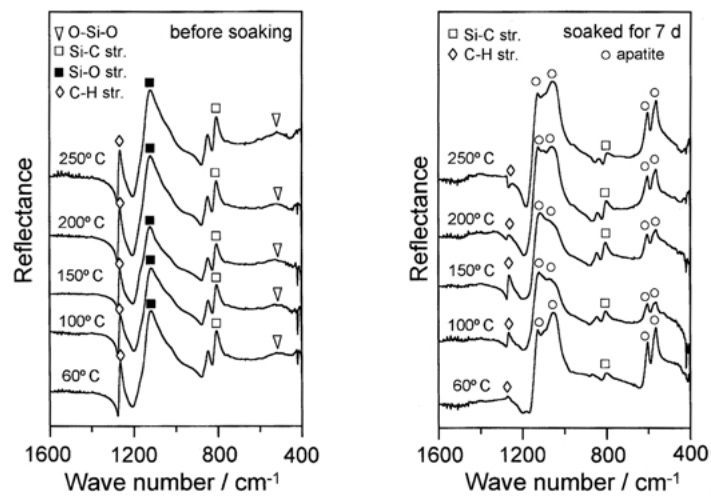


Figure 5 FTIR reflection spectra from the surfaces of the products heat treated at various temperatures before and after soaking in SBF for seven days.

The product heat treated at 60 °C formed the apatite on its surface in SBF within only one day and those heat treated at 100 °C–250 °C did within three days, as shown in Figs 4 and 5, as well as Table I. These indicate that they form the apatite on their surfaces, even living body, and bond to living bone through this apatite layer [18, 19]. Although the induction period for the apatite formation on the surface of the hybrid in SBF increases a little by heat treatment, the induction period for all the products is comparable to that of highly bioactive glass-ceramic A-W [17, 18, 31]. This means that all the

products are highly bioactive. Mechanism of the apatite formation in the present products is explained as follows.

The calcium ion is released from the products, as shown in Fig. 8, to exchange with H_3O^+ ion in SBF. As a result, a lot of Si-OH and Ti-OH groups are formed on the surfaces of the products, and the ionic activity product of the apatite in SBF is increased. Thus formed Si-OH and Ti-OH groups induce the apatite nucleation [32] and the increased ionic activity product of the apatite accelerates apatite nucleation. Once the apatite nuclei are formed, they grow spontaneously by con-

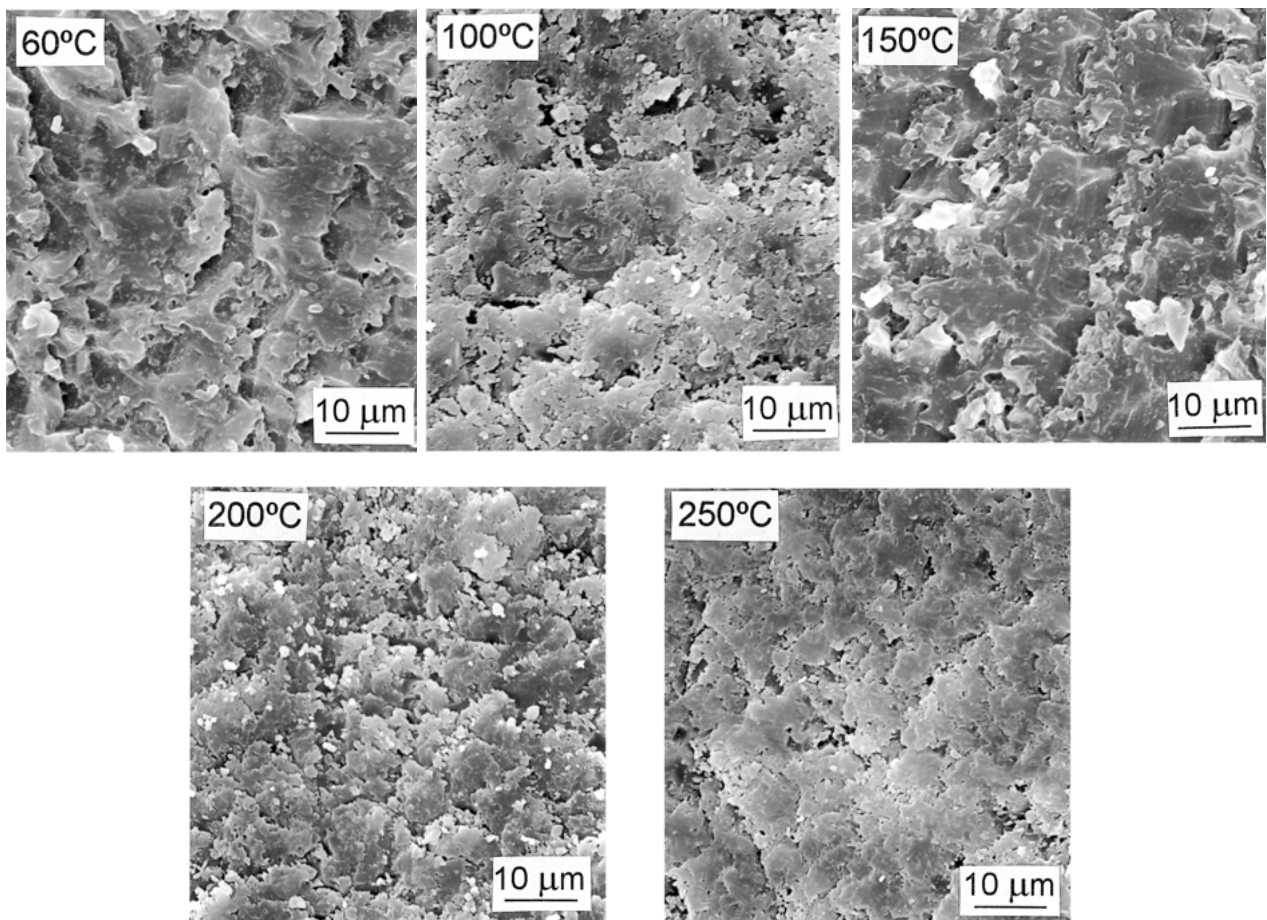


Figure 6 SEM photographs of the surfaces of the products heat treated at various temperatures.

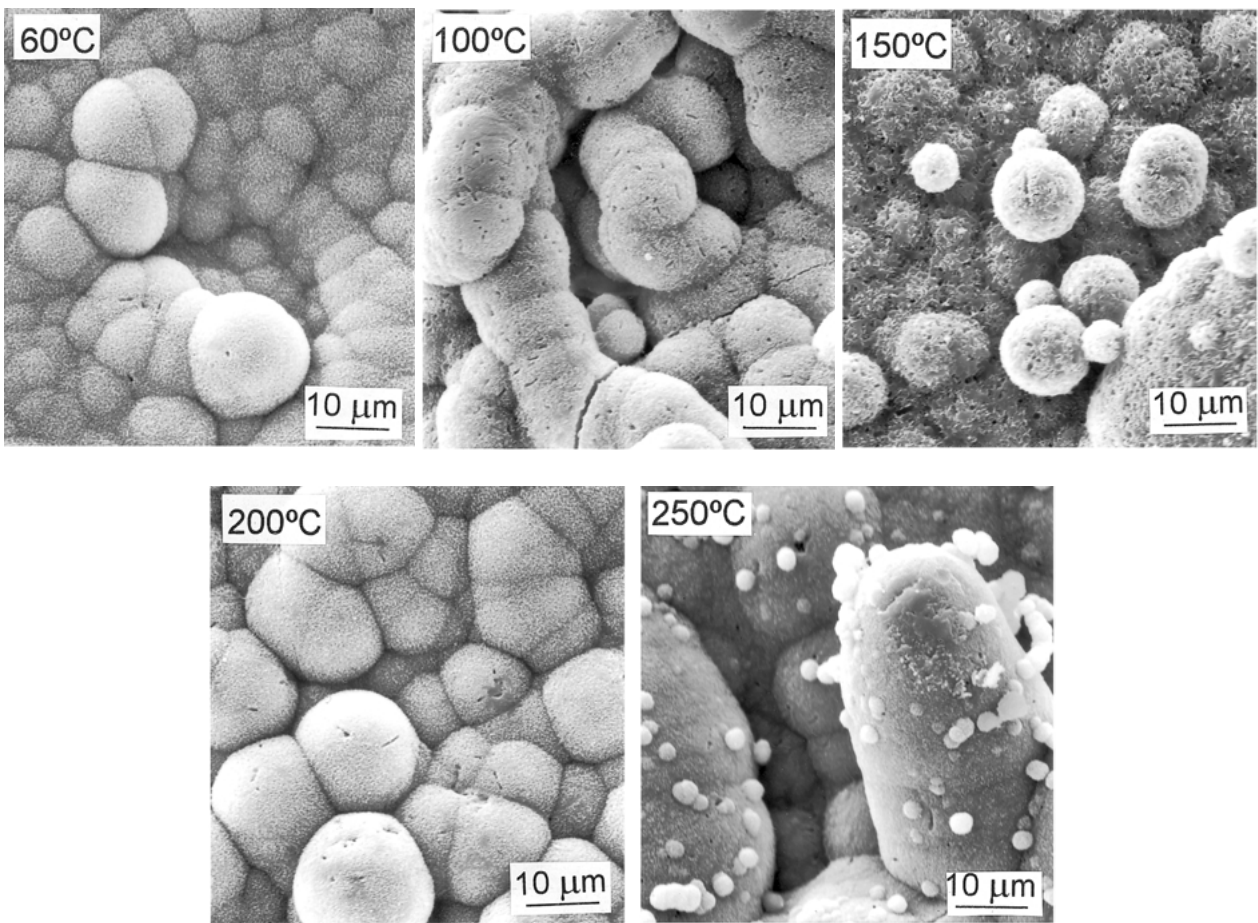


Figure 7 SEM photographs of the surfaces of the products heat treated at various temperatures after soaking in SBF for seven days.

suming the calcium and phosphate ions from SBF, thereby the decrease in phosphorous concentration in SBF occurs as shown in Fig. 8.

It should be noted that the release of the silicon ion from the products decreases with increasing heat treatment temperature. This indicates that chemical durability of the products increases with increasing heat treatment temperature. This might be attributed to the formation of a compact structure of the Si-O-Ti network, due to decrease in the content of PDMS.

It is apparent from Fig. 9 that all the present products show a certain degree of capability for deformation. The magnitude of the strain at failure decreases with increasing heat treatment temperature, and its values went down to those exhibited by the human cancellous

bone (5–7%) [27] in the range of heat treatment temperature from 150 to 250 °C. The decrease in the failure strain with increasing heat treatment temperature is attributed to the reduction of the PDMS content by the heat treatment. The bending strengths of the products were about 11 MPa, independent of the heat treatment temperature, which are comparable to those of human cancellous bone [27]. The Young's modulus of the products increased with increasing heat treatment temperature. This might be attributed to the formation of compact structure by the heat treatment. All these values fell in the range of those exhibited by the human cancellous bone (see Fig. 10).

It can be seen from these results that dense and transparent bioactive PDMS-modified CaO-SiO₂-TiO₂

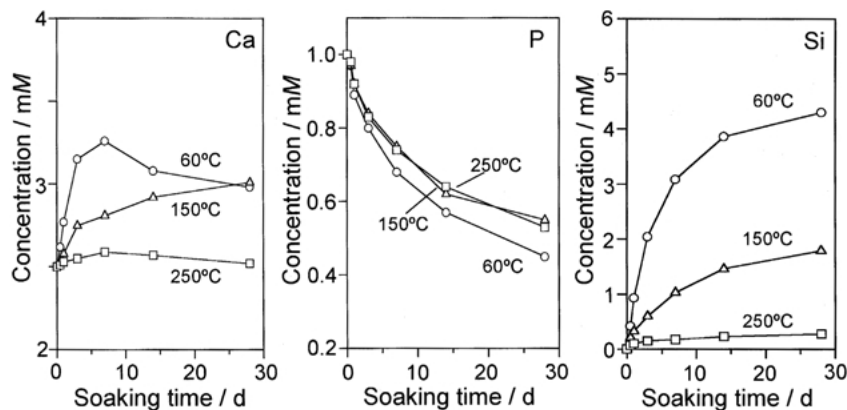


Figure 8 Changes in element concentrations of SBF due to soaking of the products heat treated at 60, 150 and 250 °C.

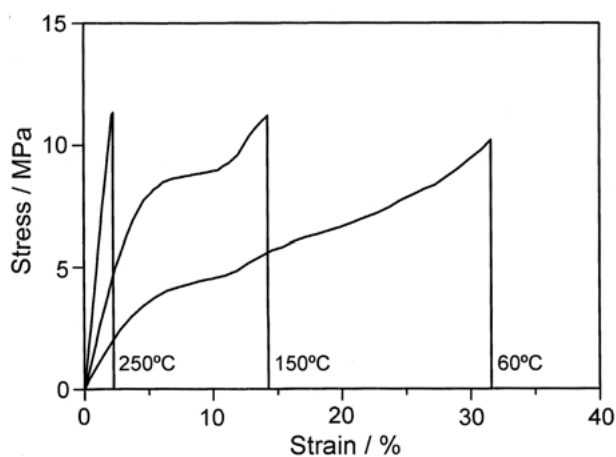


Figure 9 Stress versus strain curves of the products heat treated at 60, 150 and 250 °C, measured by three-point bending test.

hybrid materials with high extensibilities and low Young's moduli are obtained by the hydrolysis and polycondensation of PDMS, TEOS, TiPT and calcium nitrate. Their strain at failure and Young's modulus decreased and increased, respectively, with increasing heat treatment temperature up to 250 °C without showing a large change in transparency, bioactivity and bending strength. Thus, highly bioactive hybrids with mechanical properties analogous to those of the human cancellous bone were obtained.

5. Summary

Hydrolysis and polycondensation of PDMS, TEOS, TiPT and calcium nitrate gave essentially pore- and crack-free transparent monolithic products. They were considered to be composed of a Si-O-Ti-O network modified with methyl groups and calcium ion ionically bonded to the network. They formed an apatite on their surface in SBF within one to three days. Their apatite-forming ability decreased only a little with a heat treatment up to 250 °C. They showed bending strength of about 11 MPa, which is comparable to the strength of the human cancellous bone, and independent of the heat treatment. Their strain at failure decreased with the heat treatment, and attained the values almost equal to those of the human cancellous bone, when the products are heat treated in the range of 150–250 °C. Their Young's modulus increased with the heat treatment, but the values were always within the range of those of human cancellous bone. Thus, highly bioactive hybrids with mechanical properties analogous to those of the human cancellous bone were obtained. These hybrids may be useful as a new kind of bioactive bone-repairing material.

Acknowledgments

This work was supported by The Special Coordination Fund of the Science and Technology Agency of Japan, Research on Creation of Biointegrated Materials to Improve Physically Handicapped People's Quality of Life. The experiment guidance of pore volume measurements of Dr K. Nakanishi is greatly appreciated.

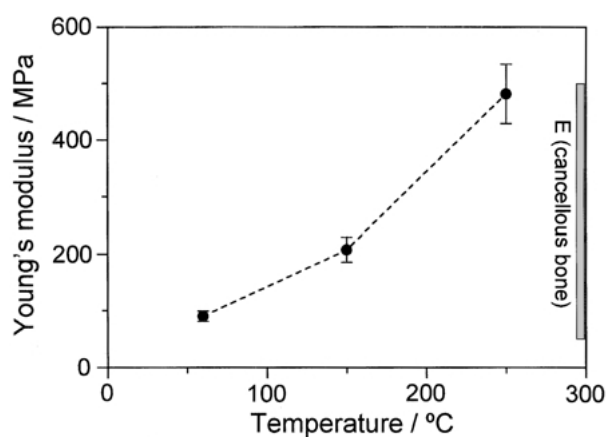


Figure 10 Young's modulus of the products as a function of heat treatment temperature. In the right-hand side, the range of Young's moduli of human cancellous bone [27] is shown for comparison.

References

1. L. L. HENCH, R. J. SPLINTER, W. C. ALLEN and T. K. GREENLEE JR, *J. Biomed. Mater. Res.* **2** (1971) 117.
2. M. JARCHO, J. L. KAY, R. H. GUMAER and H. P. DROBECK, *J. Bioeng.* **1** (1977) 79.
3. T. KOKUBO, M. SHIGEMATSU, Y. NAGASHIMA, M. TASHIRO, T. NAKAMURA, T. YAMAMURO and S. HIGASHI, *Bull. Inst. Chem. Res., Kyoto Univ.* **60** (1982) 260.
4. H.-M. KIM, F. MIYAJI, T. KOKUBO and T. NAKAMURA, *J. Biomed. Mater. Res.* **32** (1996) 409.
5. C. A. VAN BLITTERSWIJK, D. BAKKER, H. LEENDERS, J. VD BRINK, S. C. HESSELING, Y. P. BOVELL, A. M. RADDER, R. J. SAKKERS, M. L. GAILLARD, P. H. HEINZE and G. J. BEUMER, in "Bone-bonding Biomaterials", edited by P. Ducheyne, T. Kokubo and C. A. Van Blitterswijk (Reed Healthcare Communications, Leiderdorp, The Netherlands, 1992) p. 13.
6. H. SCHMIDT, *J. Non-Cryst. Solids* **73** (1985) 681.
7. G. L. WILKES, B. ORLER and H. HUANG, *Polym. Prepr.* **26** (1985) 300.
8. H.-H. HUANG, B. ORLER and G. L. WILKES, *Polymer Bulletin* **14** (1985) 557.
9. B. K. COLTRAIN, C. SANCHEZ, D. W. SCHAEFER and G. L. WILKES, (eds), in "Better Ceramics Through Chemistry VII: Organic/Inorganic Hybrid Materials", vol. 435, (Materials Research Society, Pittsburgh, 1996).
10. Y. P. NING, M. X. ZHAO and J. E. MARK, in "Chemical Processing of Advanced Materials", edited by L. L. HENCH and J. K. West (John Wiley and Sons Inc., New York, 1992) p. 745.
11. J. D. MACKENZIE, Y. J. CHUNG and Y. HU, *J. Non-Cryst. Solids* **147 & 148** (1992) 271.
12. J. D. MACKENZIE, *J. Sol-Gel Sci. Techn.* **2** (1994) 81.
13. S. MOTAKEF, T. SURATWALA, R. L. PONCONE, J. M. BOULTON, G. TEOWEE and D. R. UHLMANN, *J. Non-Cryst. Solids* **178** (1994) 37.
14. K. TSURU, C. OHTSUKI, A. OSAKA, T. IWAMOTO and J. D. MACKENZIE, *J. Mater. Sci.: Mater. Med.* **8** (1997) 157.
15. Q. CHEN, N. MIYATA, T. KOKUBO and T. NAKAMURA, *J. Biomed. Mater. Res.* **51** (1999) 605.
16. S. FORDHAM, (ed.), in "Silicones", (George Newnes Ltd, London, 1960) p. 180.
17. T. KOKUBO, H. KUSHITANI, S. SAKKA, T. KITSUGI and T. YAMAMURO, *J. Biomed. Mater. Res.* **24** (1990) 721.
18. T. KOKUBO, *Biomaterials* **12** (1991) 155.
19. L. L. HENCH, *J. Am. Ceram. Soc.* **74** (1991) 1487.
20. G. ORCEL, J. PHALIPPOU and L. L. HENCH, *J. Non-Cryst. Solids* **88** (1986) 114.
21. D. L. OU and A. B. SEDDON, *ibid.* **210** (1997) 187.
22. A. CHMEL, G. M. ERANOSYAN and A. A. KHARSHAK, *ibid.* **146** (1992) 213.
23. S. DIRE and F. BABONNEAU, *J. Sol-Gel Sci. Techn.* **2** (1994) 139.
24. X. LI and T. A. KING, *J. Non-Cryst. Solids* **204** (1996) 235.
25. R. M. SILVERSTEIN, G. C. BASSLER and T. C. MORRILL,

- (eds), in "Spectrometric Identification of Organic Compounds", (John Wiley & Sons, Inc., New York, 1981).
26. I. REHMAN and W. BONFIELD, *J. Mater. Sci.: Mater Med.* **8** (1997) 1.
 27. L. L. HENCH and J. WILSON, (eds) in "An Introduction to Bioceramics", (World Scientific Publishing Co., Singapore, 1992), p. 12.
 28. H. H. HUANG, B. ORLER and G. L. WILKES, *Macromolecules* **20** (1987) 1322.
 29. T. IWAMOTO, K. MORITA and J. D. MACKENZIE, *J. Non-Cryst. Solids* **159** (1993) 65.
 30. Y. HOSHINA and J. D. MACKENZIE, *J. Sol-Gel Sci. Techn.* **5** (1995) 83.
 31. T. KOKUBO, S. ITO, Z. T. HUANG, T. HAYASHI, S. SAKKA, T. KITSUGI and T. YAMAMURO, *J. Biomed. Mater. Res.* **24** (1990) 331.
 32. P. LI, C. OHTSUKI, T. KOKUBO, K. NAKANISHI, N. SOGA and K. DE GROOT, *ibid.* **28** (1994) 7.

*Received 30 December 1999
and accepted 2 March 2000*